RSC Advances

This article can be cited before page numbers have been issued, to do this please use: E. Rafiee, M. Joshaghani and P. Ghaderi-Sheikh Abadi, *RSC Adv.*, 2015, DOI: 10.1039/C5RA14467A.

View Article Online
DOI: 10.1039/C5RA14467A

Journal Name

ARTICLE

Received 00th January 20xx,
Accepted 00th January 20xx

DOI: 10.1039/x0xx00000x

www.rsc.org/

Shape-dependent Catalytic Activity of Fe_3O_4 Nanostructures under the Influence of External Magnetic Field for the Multicomponent Reactions in Aqueous Media

E. Rafiee,[a,b]† M. Joshaghani[a,b] and P. Ghaderi-Shekhi Abadi[b]

High-quality and high-active one-dimensional (1-D) Fe_3O_4 nanostructure was synthesized *via* the external magnetic field (EMF) at intensity range 0–526 μT in aqueous solution, without using any surfactant and organic solvent at room temperature. Characterization of the products were carried out using scanning electron microscopy (SEM), energy dispersive X-ray spectroscopy (EDX), X-ray diffraction spectroscopy (XRD), Fourier transform infrared spectrophotometry (FT-IR), laser particle size analyzer, surface area (Brunauer-Emmett-Teller, BET), and vibrating sample magnetometer (VSM). The results show that EMF at a critical adjusted intensity has a great influence on the structural features such as the morphology, particle size, surface pores size distribution, and magnetic properties of the Fe_3O_4 nanostructure. The morphology changed from peg-like network structures to needle-like cage structures by exposure synthesis treatment with EMF at intensity 362 μT. The catalytic activity of two nanostructures prepared in the presence and absence of EMF were compared in tricomponents reaction (TCR) for the synthesis of trisubstituted imidazoles under electromagnetic irradiation. The best results were obtained for the catalyst produced in the presence of EMF while the tricomponent reaction carried out in the absence of EMF. This EMF conditions was used for preparation of a series of alkyl–, aryl–, and heteroaryl–substituted imidazoles from the corresponding benzoin and benzil in aqueous solution as green reaction conditions. It was found that the catalyst can be efficiently recycled and reused for several repeating cycles without significant loss of catalytic activity.

Introduction

Tuning of magnetization is important technology in the synthesis of magnetic material. The tuning of magnetization typically has been achieved by external magnetic field (EMF- template-free) generated from electromagnets. Recent developments have indicated that the magnetic field, as an elegant way, could be applied to orient magnetic material into nano- or microscale structures in which dipole interactions between adjacent magnetic particles couple them together and force the reversible formation of an anisotropic structure.[1–4] Anisotropic nanostructures have attracted wide spread attention in the past decades owing to their unique electronic, magnetic, and optical properties in various applications.[5–8] In particular, the controlled synthesis of multi-dimensional (M-D) metallic nanostructures is one of the research hotspots, as anisotropic morphologies can dramatically influence their physical and chemical properties,[9] for example, 1-D magnetic materials have technological applications by specific properties.[10–16] It is known that magnetic materials possess easy magnetic axes. For example, Fe_3O_4 has easy magnetic axes along the (111) and (110) directions[17] under external magnetic field to form 1-D nanostructures of magnetic materials. Dimensional orientation can be tuned magnetic properties of the materials. Many efficient techniques were developed for preparing the 1-D Fe_3O_4 structures, mainly including template-assisted strategy.[18,19] However, the preparation and removal of a template are difficult tasks in some cases.[18] Template-free strategies are always of great interest, since the post-treatment of linear templates may have a bad effect on the magnetic and electronic properties of the resulting structures.[20]

According to previous researches, the magnetic field can be influence not only the synthesis of magnetic materials but also on the organic reactions,[21–27] but these researches mainly focused on the synthesis of magnetic materials under EMF and the nonmagnetic materials by this strategies. In the present work, different Fe_3O_4 catalysts were prepared under various magnetic field conditions as the magnetic catalysts. Reactivity of the produced catalyst was also investigated in tricomponent reactions (TCRs) of 1, 2– diketones, benzaldehyde, and ammonium acetate in water as green reaction conditions.

Scientists have made great achievements in M-D nanostructures of magnetic elements.[28–32] To the best of our knowledge, there are

---

[a] *Department of Inorganic Chemistry, Faculty of Chemistry, Razi University, Kermanshah, 67149, Iran.*

[b] *Institute of Nano Science and Nano Technology, Razi University, Kermanshah, 67149, Iran.*

† Corresponding author: Tel./Fax: +98 833–4274559; E-mail: ezzat_rafiee@yahoo.com, e.rafiee@razi.ac.ir.

Electronic Supplementary Information (ESI) available: [details of any supplementary information available should be included here]. See DOI: 10.1039/x0xx00000x

View Article Online
DOI: 10.1039/C5RA14467A

few reports on the effect of magnetic field in chemical reactivity of the process while competitive factors exist in the reaction system.[33–37] The effect of different reaction conditions including of an EMF on the TCR (Scheme 1) have been investigated. The TCR is promoted by the synthesis of magnetic materials in the presence and absence of EMF to derive a novel reaction condition that possesses both adequate yield and reaction time. In this paper, four different reaction types (Scheme 1) will be contrasted together.

Results and discussion

Catalytic behaviour

During our initial studies, to investigate the EMF effect on the synthesis of magnetic catalysts and main organic reaction, the ZEMF and AEMF1 (according to Table 1) were chosen as catalysts and the model reaction (Scheme 1) was carried out in the presence and absence of the EMF. Based on our recent success for the synthesis of imidazoles,[33] same experimental protocol for the synthesis of trisubstituted imidazoles was employed. A solvent-free condition was chosen as the reaction environment at 80 °C using 0.0025 g of the magnetic catalyst. Therefore, four different reaction types were obtained in the reaction of benzil, benzaldehyde, and NH_4OAc as model reaction (Scheme 1 and Table 2).

Table 1 Experimental conditions for preparation of different Fe_3O_4 catalysts.

Entry	Symbol	EMF intensity (μT)	Morphology of the products
1	ZEMF[a]	0	Peg-like network
2	AEMF1	362	Needle-like network
3	AEMF2	432	Aggregate structures
4	AEMF3	485	Stacked leafs
5	AEMF4[b]	362	Rod-like particle
6	AEMF5[c]	362	Purposeful nanorods
7	AEMF6[d]	362	Cotton-like structure

[a] Reaction time = 40 min.
[b] Preliminary treatment exposure the reaction solution by EMF.
[c] Terminally treatment exposure the reaction solution by EMF.
[d] Pulsed magnetic field exposure the reaction solution.

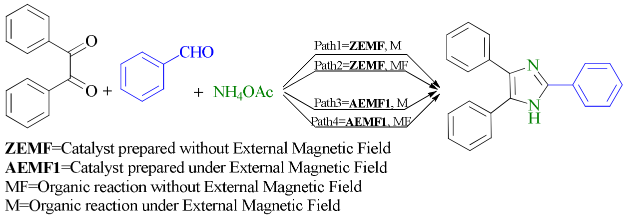

Scheme 1 Different reaction conditions.

With the using of ZEMF as catalyst at the presence of 432 μT of the EMF, only 36% product yield was obtained after 10 min but with the using of ZEMF catalyst in 80 °C without using any EMF, the 95% yield was obtained in longer reaction time (Table 2, entries 1 and 2). According to the results of entries 3 and 4 of the Table 2, it seems that using of EMF inhibits the progress of the organic reaction but AEMF1 is more efficient than ZEMF as catalyst. Thus, using catalyst which was prepared in magnetic field in the model reaction in the absence of magnetic field was chosen as the best reaction conditions (Table 2, entry 4). Possibly the agglomeration of magnetic catalysts which decrease the surface area while the reaction proceeds at EMF is the original reason for lower activity when reaction carried out in magnetic field. Thus, in other experiments, organic reactions were carried out in the absence of magnetic field but magnetic field was used for catalyst preparation.

In next step, various parameters were investigated, such as temperature, solvent, catalyst loading, and type of the catalyst in the model reaction (Table 3).

Table 2 Investigation of the EMF effect on the model reaction.[a]

Entry	Catalyst type	Magnetic field	Time (min)	Yield (%)[b]
1	ZEMF	M[c]	10 (50)	36 (35)
2	ZEMF	MF[d]	50 (70)	60 (95)
3	AEMF1	M[c]	5 (50)	35 (37)
4	AEMF1	MF[d]	50	95
5	AEMF1	MF[e]	50 (3 h)	20 (70)

[a] Reaction conditions: benzil, (1.0 mmol); benzaldehyde, (1.0 mmol); NH_4OAc, (2.0 mmol); solvent-free; catalyst, (0.0025 g); at 80 °C.
[b] Isolated yield.
[c] EMF intensity = 432 μT.
[d] Magnetic field free, T = 80 °C.
[e] Room temperature.

In the first set of experiments 0.0025 g of AEMF1 as catalyst was used in solvent-free conditions, and four different temperatures were evaluated (Table 3, entries 1–4). In all of these experiments the desired product was obtained, with yields ranging from 90 to 94% but when the reaction was performed in 60 °C the expected trisubstituted imidazole was afforded in lower reaction time compare with 30 and 40 °C (Table 3, entry 3). Recently, the development of new strategies for using water as solvent in organic reaction has stimulated interest among the synthetic community since it avoid environmental issues arising from the use of organic solvents. Excellent yield was obtained at very short reaction time in water as solvent (Table 3, entry 5). It should be noted that amount of AEMF1 as catalyst has an influence on the product formation. There was a slight decrease in the yield of the corresponding product from 98 to 94% when the amount of AEMF1 catalyst was changed from 0.0025 to 0.003 g but there was a high decrease in the reaction time from 25 to 10 min. No significant alteration was verified using 0.004 g of AEMF1 as catalyst (Table 3, entries 6–8).
According to the results presented in Table 1, since AEMF1 (which was synthesized in the presence of EMF) shows excellent catalytic activity in the model reaction, influence of different EMF intensity was investigated in the catalyst synthesis process and catalytic activity of these catalysts was studied in model reaction (Table 3, entries 7 and 9–14). It seems that AEMF1 and AEMF6 as catalysts showed the best performance (Table 3, entries 7 and 13). Because the synthetic procedure of the AEMF6 is tedious and not technically simple (as discussed in Experimental section) AEMF1 was chosen as the best catalyst. In the other hand, magnetic-free (ZEMF) catalyst exhibited similar activity with AEMF1 at very longer reaction time which indicates predictable role of EMF as promoter and resister in the activity of catalyst sites (Table 3, entry 14). Catalytic activity of

View Article Online
DOI: 10.1039/C5RA14467A

bulk Fe_3O_4 was investigated for comparison (Table 3, entry 15). In the absence of the catalyst, no product was formed after 10 h in optimized reaction conditions (Table 3, entry 16).

Table 3 Optimization of reaction conditions.[a]

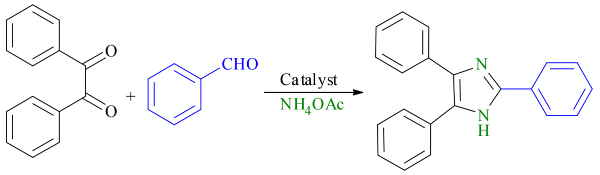

Entry	Catalyst (g)	Tem.(°C)	Solvent	Catalyst type	Time (min)	Yield (%)[b]
1	0.0025	30	Solvent-free	AEMF1	60 (7 h)	35 (90)
2	0.0025	40	Solvent-free	AEMF1	60 (7 h)	41 (92)
3	0.0025	60	Solvent-free	AEMF1	50	92
4	0.0025	80	Solvent-free	AEMF1	50	94
5	0.0025	60	H_2O	AEMF1	25	98
6	0.0015	60	H_2O	AEMF1	35	97
7	0.003	60	H_2O	AEMF1	10	94
8	0.004	60	H_2O	AEMF1	8	98
9	0.003	60	H_2O	AEMF2	23	85
10	0.003	60	H_2O	AEMF3	35	51
11	0.003	60	H_2O	AEMF4	20	94
12	0.003	60	H_2O	AEMF5	30	87
13	0.003	60	H_2O	AEMF6	7	89
14	0.003	60	H_2O	ZEMF	70	93
15	0.003	60	H_2O	Fe_3O_4 (bulk)	30 (2 h)	5 (38)
16	-	60	H_2O	None	10 h	-

[a] Reaction conditions: benzyl, (1.0 mmol); benzaldehyde, (1.0 mmol); NH_4OAc, (2.0 mmol); 1.0 mL H_2O.

[b] Isolated yield.

Characterization of the catalysts

According to Table 3, the synthetized catalysts under difference EMF conditions showed the different catalytic activities in the model reaction. Therefore we are interested to investigate reasons of the phenomena by the SEM analysis.

Under EMF (362 μT intensity) due to the dipolar interactions, leading to 1-D configuration with the ripening interaction process, alongside 1-D structures connected successively and the needle-like network was formed (AEMF1 catalyst, Fig. 1a and b). We have carried out a similar experiment without using an EMF, and the peg-like network of Fe_3O_4 is obtained, as shown in Fig. 1c and d. According to SEM images, AEMF1 exhibits the remarkably high density compare with structures of the ZEMF, which can dependence with catalytic activities of these two catalyst types (Table 3, entries 7 and 14). The results indicated that an EMF is helpful for higher aggregation of the product because the growth rate of nuclei under EMF increases. It can be seen that the connected 1-D structures increase with increasing EMF intensity to 432 μT and the aggregate structure formation (AEMF2 catalyst, Fig. 1e and f). Moreover, when the intensity of EMF is increased, the locally induced magnetic field is enhanced too and the stacked leafs were appeared (AEMF3 catalyst). The fracture edges of the Fe_3O_4 structures displayed a well-packed layered structure through the cross section (Fig. 1g and h respectively).

Fig. 2a-e shows typical low and high-magnification SEM images of the Fe_3O_4 nanostructures under different EMF conditions (preliminary, terminally, and pulsed exposure the reaction solution by EMF). Morphology of the Fe_3O_4 nanostructures obtained at preliminary exposure by EMF is that of the disarrangement rod-like particles with average diameter and length about 60 nm and 1.7 μm, respectively (AEMF4 catalyst, Fig. 2a and b). If the magnetic nuclei were synthesized first and then the EMF was used, the density of nanorods would decrease (AEMF5 catalyst, Fig. 2c and d). With pulsed exposure by EMF the cotton-like structures were appeared with good monodispersity (AEMF6 catalyst, Fig. 2e). According to SEM images pulsed exposure by EMF plays the force role in promoting the formation of special morphology which seems affect the catalytic activity (Table 3, entry 13).

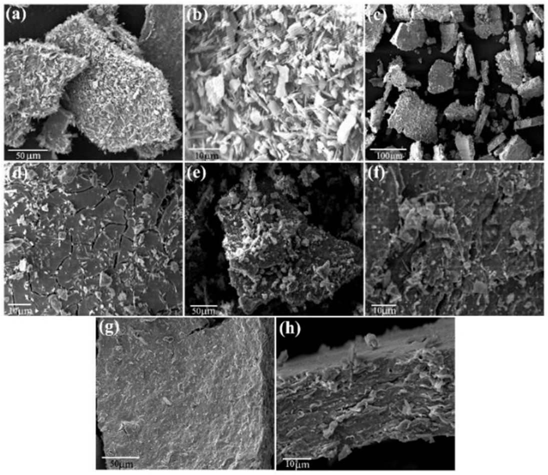

Fig. 1 SEM images of (a, b) AEMF1, (c, d) ZEMF, (e, f) AEMF2, and (g, h) AEMF3.

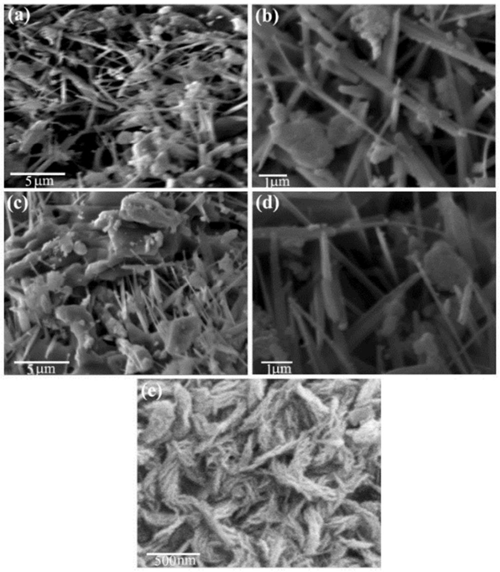

Fig. 2 SEM images of (a, b) AEMF4, (c, d) AEMF5, and (e) AEMF6.

View Article Online
DOI: 10.1039/C5RA14467A

The phase and crystalline changes, and purity of the synthetic catalysts under different EMF conditions were characterized by XRD (Fig. 3a). The magnetic catalysts (except AEMF6) have crystalline structures with peaks appearing at 29.90 °, 35.30 °, 42.50 °, 53.82 °, and 62.44 °, correspond to the (220), (311), (400), (422), and (440) planes. The peak positions are the same as reported peaks in the standard file (JCPDS card: 00–65–3107) of Fe_3O_4. The reflection peak in 48.01 °corresponded to the FeO phase. This peak observed for all the synthesis catalysts under EMF. It seems that the AEMF6 was observed at the amorphous structure. The reflection peaks in 24.41 °, 33.43 °, 41.14 °, and 64.27 °, correspond to the (012), (104), (113), and (018) planes of the ZEMF catalyst can be well indexed to the α-Fe_2O_3 (JCPDS card: 00–73–0603). According to above results, the magnetic process prevented from the phase change of the Fe_3O_4 nanostructures (unlike ZEMF).[39,40] The above results revealed that growth rate of the crystal plates of the Fe_3O_4 nanostructures could be induced under EMF. The average crystallite sizes of the catalysts calculated using the Debye-Scherrer equation ($D_c = [k\lambda \,/\, (\surd\beta_{2exp} - \beta_{2inst})\cos\theta]$) from the peak width of 35.30 ° of ZEMF, AEMF1, AEMF2, AEMF3, AEMF4, AEMF5, and AEMF6 are estimated to 34.03, 23.10, 23.69, 23.57, 22.22, 20.98, and 17.20 nm, respectively. According to above results, this found that the size of the magnetic nanocatalysts is influenced by the EMF, but intensity of the EMF shows no influence in the size of the particles.

It is considered that the synthetic catalysts under different EMF conditions indicated the different morphology and crystalline structure that these lead to the different catalyst activities. Especially the AEMF1 catalyst indicated the high catalytic activity in the model reaction. Therefore we have focused on the AEMF1 as catalyst for further characterization. The hydrodynamic size of the AEMF1 catalyst is about 25.76 nm with PDI (Polydispersity Index) of 0.225 measured by laser particle size analyzer, meaning that low aggregation in colloidal suspensions was existed in catalyst. Fig. 3b shows elemental mapping images obtained by EDX for the AEMF1 catalyst.

The FT-IR spectra of the AEMF1 catalyst is shown in Fig. 4a. The AEMF1 catalyst shows the strong absorption in the region 574 cm^{-1} corresponds to the metal-oxygen (Fe–O) stretching of Fe_3O_4.[41] Moreover, the relatively high intensity of this peak indicates the purity level and the prevalence of very small amount of defects.[42]

From the results of XRD and FT-IR analysis, it is suggested that synthesis under EMF allow forming very stable Fe_3O_4 particles without other metal oxide impurities.

The M-H loop of the as-prepared Fe_3O_4 AEMF1 was measured at room temperature (Fig. 5). The specific saturation magnetization (M_s) of the nanocatalyst is 7.32 emu/g. Reducing of M_s under EMF is same as offer results of the literature[43] (M-H loop of ZEMF was presented for comparison in Fig. 5). Furthermore, the high shape anisotropy of 1-D structures in AEMF1 would prevent needle magnetizing in directions other than along their easy magnetic axes. Despite reduced M_s, the retrieving of magnet material is still alive. This phenomena activated by high magnetic field may open up a new way to endow nanomaterials with special magnetic properties.

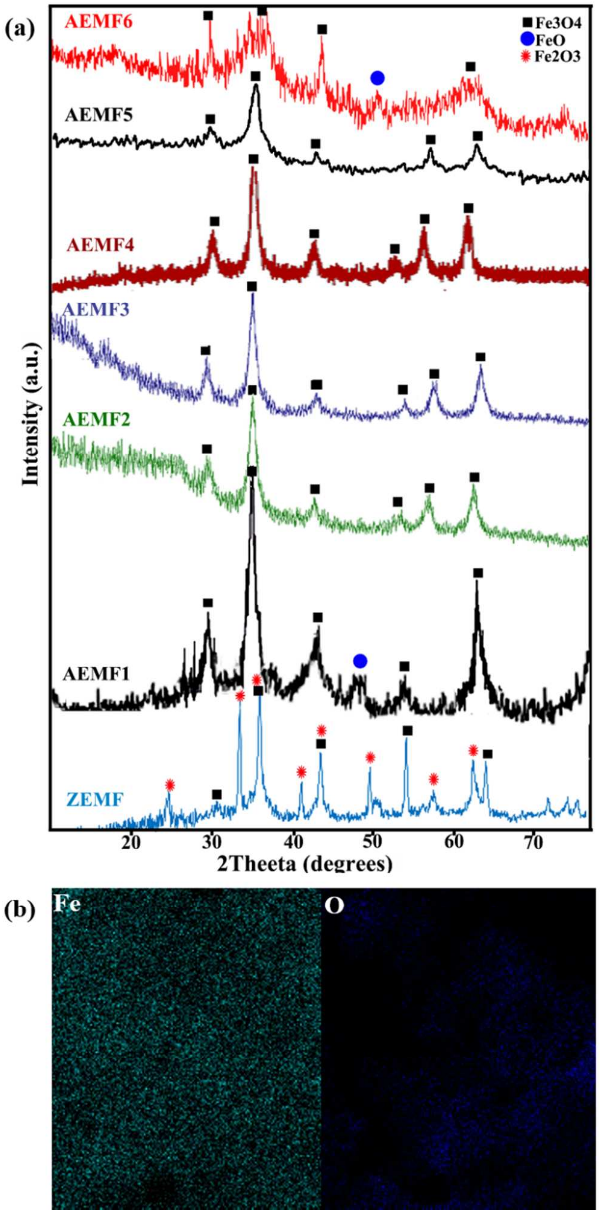

Fig. 3 (a) XRD patterns of ZEMF, AEMF1-AEMF6 and (b) EDX spectrum of the AEMF1 catalyst.

Furthermore BET test was also performed. The result made it clear that an applied magnetic field for the synthetic catalyst produced a pronounced increase in the BET specific surface area. The AEMF1 exhibits the remarkably high BET value of 101.52 m^2/g compare to BET specific surface area of ZEMF (23.02 m^2/g). May be this is the main reason for higher catalytic activity of AEMF1 (Table 3, entry 7 and 14).

View Article Online
DOI: 10.1039/C5RA14467A

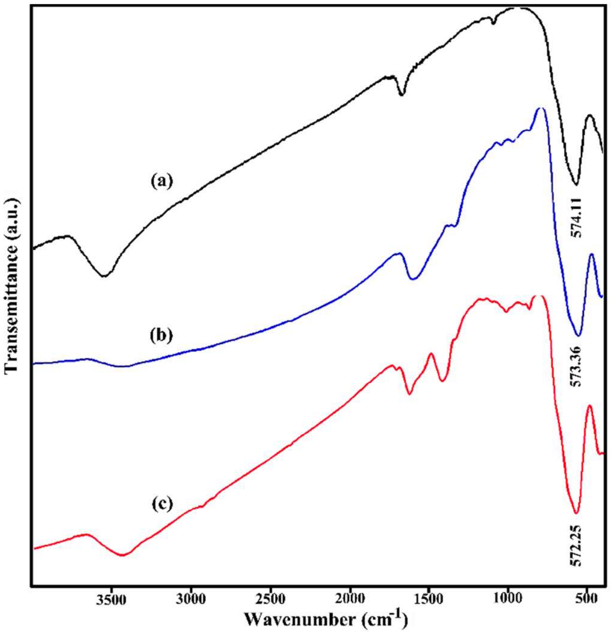

Fig. 4 FT-IR spectra of AEMF1 (a) fresh catalyst, (b) after first run, and (c) seventh run of model reaction.

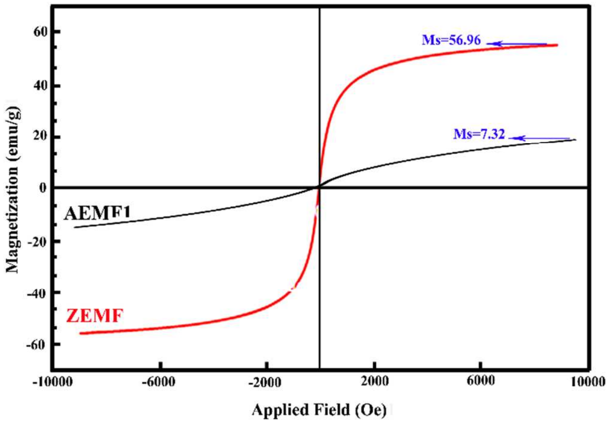

Fig. 5 Magnetization measurements of AEMF1 and ZEMF catalysts.

Synthesis of various trisubstituted imidazoles

The above results demonstrated that the AEMF1 catalyst under optimized conditions can achieve excellent yield of the trisubstituted imidazoles. A broader range of aldehydes and 1, 2-diketones was investigated in order to evaluate the scope and limitations of the method as presented in Table 4. In general, the reactions are very clean with high yielding and indicating this reaction is sensitive to electronic and steric properties of the alkyl–, aryl–, or heteroaryl–substituents.

When benzoin was used instead of benzil comparable yield was obtained with longer reaction time (Table 4, entries 1 and 2). Therefore according to these results, the benzil was selected as 1, 2– diketone source for more investigations in the synthesis of trisubstituted imidazoles. Various electron donating and withdrawing groups at the *orto*, *meta*, and *para*-position of the aryl aldehydes were used and afforded high yields (Table 4). Formation of hydrogen bond between the hydroxide and carbonyl present on the salicylaldehyde does not effect on the yield of corresponding product (Table 4, compare entries 1 and 12 as an example).[44,45] In the case of sterically demanding groups of the aryl aldehydes yields of the corresponding products were acceptable (Table 4, entries 9, 17, 19, and 21). Benzo[d]imidazole was functionalized with 2, 3, 4, 5, 6– pentafluoro phenyl (Table 4, entry 19) was also synthesized but in reflux conditions. 2– (2, 3, 4, 5, 6–Pentafluoro phenyl)-1H-benzo[d]-imidazole is an attractive building block for the synthesis of new organic fluorine semiconductors.[46] It was observed that there is a slight decrease in the product yield as the carbon length chain was increased in the case of the alkyl aldehydes (Table 4, entries 25–27).

Table 4 Preparation of trisubstituted imidazoles from 1, 2– diketones and aldehydes catalyzed by AEMF1 as catalyst.[a]

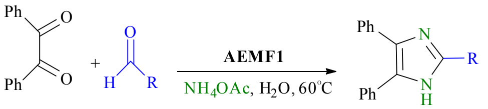

Entry	Product	Time (min)	Yield (%)[b]	Ref.
1		10	95	[47]
2[c]		30	91	[47]
3		20	89	[48]
4		5	85	[48]
5		15	92	[49]
6		15	93	[50]
7		30	88	[51]
8		20	90	[51]
9		90	72	[52,50]

View Article Online
DOI: 10.1039/C5RA14467A

10	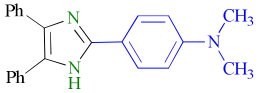	35	83	[48]
11	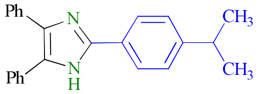	25	86	[49,50]
12	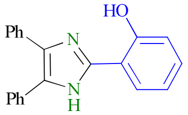	10	98	[48]
13	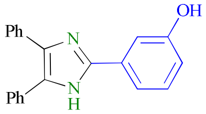	20	92	[53]
14	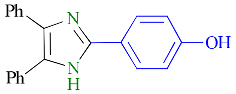	10	90	[48]
15	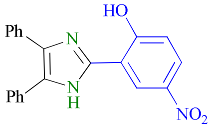	20	84	[48]
16	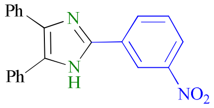	30	95	[48]
17	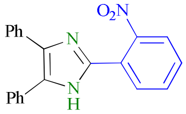	40	93	[48]
18	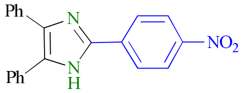	20	98	[44]
19[d]	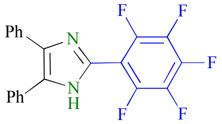	9 h	93	-
20	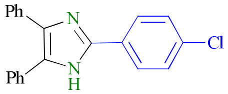	35	81	[47]
21	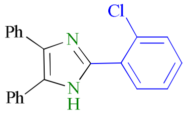	50	84	[48]
22	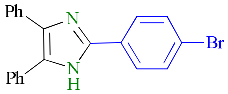	25	90	[54]
23	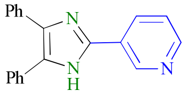	5	96	[50]
24	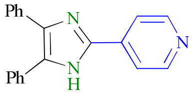	15	86	[50]
25	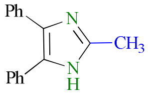	30	90	[48]
26	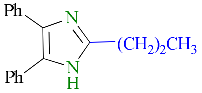	55	76	[55]
27	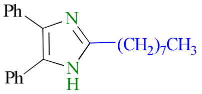	120	67	[56]

[a] Reaction conditions: the AEMF1, (0.003 g); benzil, (1.0 mmol); aldehyde, (1.0 mmol); NH_4OAc, (2.0 mmol); 1.0 mL H_2O; T = 60 °C.
[b] Isolated yield.
[c] The AEMF1, (0.003 g); benzoin, (1.0 mmol); aldehyde, (1.0 mmol); NH_4OAc, (2.0 mmol); 1.0 mL H_2O; T = 60 °C.
[d] The reaction performed at reflux conditions.

In comparison with other homogeneous and heterogeneous catalysts used in the synthesis of trisubstituted imidazoles, the AEMF1 catalyst shows remarked higher activity in shorter reaction times (Table 5).

Table 5 Comparison of the activity of the AEMF1 with other homogeneous and heterogeneous catalysts used in model reaction.

No.	Catalyst	Reaction conditions/T (°C)	Time (min)/Yield (%)	Ref.
1	Bioglycerol-based carbon catalyst	CH_3CN/55	10/84	[52]
2	HOAc	Flow microreactor system under pressure/180	2/93	[57]
3	Silica-bonded S-sulfonic acid	Solvent-free/130	80/95	[58]
4	Wang resin	AcOH/100	20 h/56	[59]
5	HOAc	Microwave irradiation/160	5/98	[60]
6	Sulfamic acid-Fe_3O_4	Ultrasound irradiation/40	25/98	[61]
7	InF_3	Solvent-free/60	26/91	[62]
8	HBF_4-SiO_2	Neat/120	15/92	[63]
9	$InCl_3.3H_2O$	MeOH/30	8.3 h/82	[64]
10	Silica sulfuric acid	Solvent-free/130	50/83	[65]
11	L- Proline	MeOH/60	9 h/90	[48]
12	Y(OTF)3	$C_{10}F_{18}$/80	6 h/80	[55]
13	Nano SBA-15	2, 2, 2-Trifluoroethanol/90	3 h/92	[47]
14	Fe_3O_4	H_2O/60	10/95	Present work

Reusability of the magnetic catalysts

Finally, the AEMF1 catalyst was recyclable very easy with slight loss of activity. In order to facilitate the catalyst recovery the runs were made in tenfold scale. We consider the loss of catalyst during the recovery process was 3 wt.% after seventh run. After completion of the reaction, the catalyst was recovered from the reaction mixture by external magnet and reused for the fresh reaction. It was found that the AEMF1 catalyst could be reused at least seven times with a slight decrease in activity (Fig. 6). According to the FT-IR spectra in Fig. 4b and c, it seems that magnetic catalyst is stable in the reaction and recovery process at least after seven reusing.

View Article Online
DOI: 10.1039/C5RA14467A

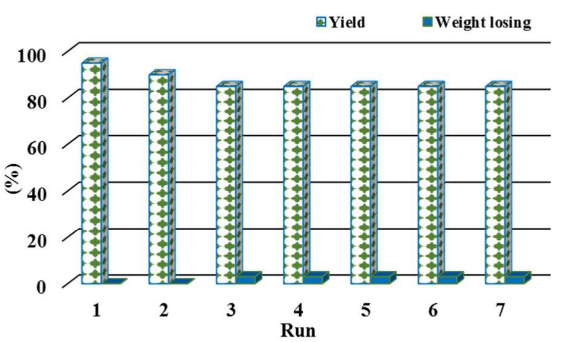

Fig. 6 Recycling test of the AEMF1 catalyst and weight losing in model react ion after 10 min.

Mechanism of the reaction

The plausible mechanism (Scheme 2) for the synthesis of corresponding imidazole in model reaction in the presence of AEMF1 involves the initial interaction of AEMF1 with aldehyde leading to the formation of intermediate (I), which attacked by the amine source gives another intermediate (II). This intermediate reacts with amine source generating intermediate (III). Intermediate (III) at the presence of AEMF1 reacted with benzil and leads to the desired product.[66–68]

Conclusions

Fe_3O_4 nanostructure has been synthesized in the presence of EMF as an efficient and stable catalyst. EMF provide a good opportunity to design 1-D Fe_3O_4 with high surface area. This magnetic catalyst showed excellent activity in the synthesis of trisubstituted imidazole with easy separation from the reaction mixture using EMF along with organic process do not increased the catalytic activity of magnetic catalyst. The catalyst could be recovered and reused at least seventh times without significant decreasing in catalytic activity. This study is an initial attempt toward synthesis of the 1-D Fe_3O_4 nanostructures. Modification of synthetic approach and preparation, properties, and application in a wide range of other chemical reactions are in progress and will be reported in due course.

Experimental

Material and methods

Analytical grades of $FeCl_3.6H_2O$, $FeCl_2.4H_2O$, NaOH, 1, 2–diketones, aldehydes, and NH_4OAc were purchased from Merck and were used without further purifications. The magnetic field was generated by a Helmholtz cylinder permanent magnet and fuel source. The bore diameter was 3 cm, and a magnetic flux density of range of 362 to 526 μT could be imposed. ^{1}H and ^{13}C NMR spectra were recorded on a Bruker Avance 200 MHz NMR spectrometer with $CDCl_3$ as solvent and TMS as internal standard. The FT-IR spectra of the samples were recorded at room temperature using a Bruker, ALPHA spectrophotometer at a spectral resolution of 4 cm^{-1} using KBr pellets in the range of 400–4000 cm^{-1} with a delicate beam condenser and a liquid nitrogen cooled MCT-detector. XRD patterns were recorded by an Inel French, EQUINOX 3000 model X-ray diffractometer using Cu K_α radiation. Scanning electron microscopy (SEM) has been performed using an AIS2300C microscope with scanning range from 0 to 20 keV. Energy dispersive X-ray (EDX) measurements were made with an IXRF model 550i attached to SEM. SEM/EDX samples were prepared by coating of solid particles into a conductive layer. The size distribution of the samples was obtained using a laser particle size analyzer (HPPS5001, Malvern, UK). The magnetic properties of Fe_3O_4 nanostructure were measured using a BHV-55, Riken, Japan vibrating sample magnetometer (VSM). The specific surface area (using BET and BJH methods), the total pore volume, and the mean pore diameter were measured using a N_2 adsorption-desorption isotherm at liquid nitrogen temperature (−196 °C), using a NOVA 2200 instrument (Quantachrome, USA). Prior to the adsorption-desorption measurements, all the samples were degassed at 110 °C in a N_2 flow for 3 h to remove the moisture and other adsorbates. Thin layer chromatography on precoated silica gel Fluorescent 254 nm (0.2 mm) on aluminum plates was used for monitoring the reactions.

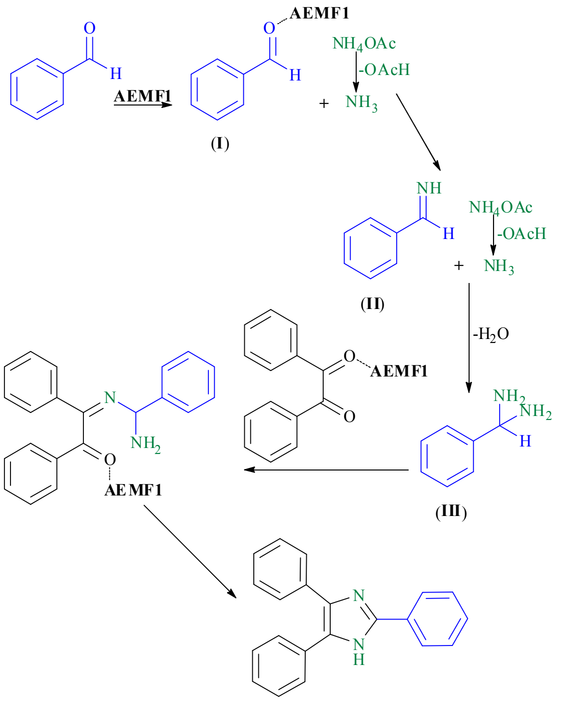

Scheme 2 Possible mechanism for the synthesis of trisubstituted imidazoles.

Preparation of the 1-D Fe_3O_4 nanostructure catalysts

In a typical procedure, $FeCl_3.6H_2O$ (0.06 mol) and $FeCl_2.4H_2O$ (0.03 mol) were dissolved into the 5.0 ml of deoxygenated water (by nitrogen gas bubbling). The resulting solution was added drop wise into 25 ml NaOH (1.5 M) under vigorous

View Article Online
DOI: 10.1039/C5RA14467A

mechanical stirring at room temperature. The overall experimental process was performed in a Helmholtz cylinder permanent magnet with a value of 362–526 μT. A black precipitate formed after 20 min. After synthesis treatment, the resulting black precipitate was collected, filtered, and washed with deoxygenated distilled water several times to remove any possible impurities, and finally dried in a desiccator at room temperature before characterization. The as-obtained crystalline Fe_3O_4 sample was denoted as the AEMF catalyst. Preparation conditions for all catalysts and their abbreviations were summarized in Table 1. For synthesis of AEMF6, a mixture of iron salts in deoxygenated water and NaOH solution was exposured by EMF (362 μT) for 5 min then the EMF was removed (the mixture of solution was stirred). This condition was repeated for four times.

General procedure for the one-pot synthesis of trisubstituted imidazoles

In a typical reaction, a suspension of benzil (1.0 mmol), aldehyde (1.0 mmol), and ammonium acetate (2.0 mmol) were added to mixture of catalyst (0.003 g) and 5 mL distilled water. The resulting mixture was heated to 60 °C for an appropriate time. In the case of exposure by EMF, the resulting mixture was transferred to a Helmholtz cylinder permanent magnet and exposed with 432 μT intensity for an appropriate time. After completion of the reaction, the mixture was cooled to room temperature and the solid (containing catalyst and product) was filtered off and washed with deoxygenated distilled water. The product was dissolved in ethyl acetate, and the catalyst was separated from the product using an external magnet. The solvent was evaporated in a *vacuum* to give the crude product, which was purified by recrystallization from ethyl acetate. All products were identified by comparing their ^{1}H NMR with those in authentic samples[44,47–56] except for new compound 2-(2, 3, 4, 5, 6-pentafluorophenyl)-4,5-diphenyl-1H-imidazole. Analytical data for this compound is presented below:

2-(2, 3, 4, 5, 6-Pentafluorophenyl)-4,5-diphenyl-1H-imidazole (Table 4, entry 19): mp: 361–362 °C; ^{1} H NMR (200 MHz, $CDCl_3$, TMS): δ (ppm): 7.19 (4H, m, CH), 7.30 (4H, m, CH), 7.48 (2H, m, CH), 12.50 (1H, brs, NH).

Other products are known and ^{1}H NMR results are reported as supplementary information.

Acknowledgements

The authors thank the Razi University Research Council for support of this work.

Notes and references

1 E.M. Furst, C. Suzuki, M. Fermigier and A.p. Gast, *Langmuir*, 1998, **14**, 7334.

2 H. Niu, Q. Chen, M. Ning, Y. Jia and X. Wang, *J. Phys. Chem. B*, 2004, **108**, 3996.

3 R. Sheparovych, Y. Sahoo, M. Motornov, S. Wang, H. Luo, P.N. Prasad, I. Sokolov and S. Minko*, Chem. Mater*. 2006, **18**, 591.

4 A.K.Vuppu, A.A.Garcia and M.A. Hayes, *Langmuir*, 2003, **19**, 8646.

5 J. Gao, H. Gu and B. Xu, *Acc. Chem. Res*, 2009, **42**, 1097.

6 L. Cademartiri and G.A. Ozin, *Adv. Mater*, 2009, **21**, 1013.

7 P. Tartaj, M.P. Morales, T. Gonzalez Carreño, S. Veintemillas Verdaguer and C.J. Serna, *Adv. Mater.*, 2011, **23**, 5243.

8 S. Laurent, D. Forge, M. Port, A. Roch, C. Robic, L. Vander Elst and R.N. Muller, *Chem. Rev.*, 2008, **108**, 2064.

9 Y. Xia, P. Yang, Y. Sun, Y. Wu, B. Mayers, B. Gates, Y. Yin, F. Kim and H. Yan, *Adv. Mater.*, 2003, **15**, 353.

10 N.A. Melosh, A. Boukai, F. Diana, B. Gerardot, A. Badolato, P.M. Petroff and J.R. Heath, *Science*, 2003, **300**, 112.

11 V.F. Puntes, K.M. Krishnan and A.P. Alivisato, *Science*, 2001, **291**, 2115.

12 J. Bao, C. Tie, Z. Xu, Q. Zhou, D. Shen and Q. Ma, *Adv. Mater*, 2001, **13**, 1631.

13 R. Hertel, *J. Magn. Magn. Mater*, 2002, **249**, 251.

14 N. Cordente, M. Respaud, F. Senocq, M.J. Casanove, C. Amiens and B. Chaudret. *Nano Lett.*, 2001, **1**, 565.

15 M. Wu, Y. Xiong, Y. Jia, H. Niu, H. Qi, J. Ye and Q. Chen, *Chem. Phys. Lett.*, 2005, **401**, 374.

16 M.J. Kim, Y.W. Kim, J.S. Lee, J.B. Yoo, C.Y. Park, C. J. Bae, J. G. Park and J. Korean, *Phys. Soc.*, 2005, **47**, 313.

17 Y. Li and G.D. Li, *Science Publishing Corporation*, 1978, 381.

18 Z. Liu, D. Zhang, S. Han, C. Li, B. Lei, W. Lu, J. Fang and C. Zhou, *J. Am. Chem. Soc.*, 2005, **127**, 6.

19 D. Zhang, Z. Liu, S. Han, C. Li, B. Lei, M.P. Stewart, J.M. Tour and C. Zhou, *Nano Lett.*, 2004, **4**, 2151.

20 S. Banerjee and S.S. Wong, *Nano Lett.*, 2002, **2**, 195.

21 H.F. Zhang and Y.P. Shi, *Anal, Chim. Acta*, 2012, **724**, 54.

22 J.D. Qiu, M. Xiong, R.P. Liang, H.P. Peng and F. Liu, *Biosens. Bioelectron*, 2009, **8**, 2649.

23 B.H. Nguyen, L.D. Tran, Q.P. Do, H.L. Nguyen, N.H. Tran and P.X. Nguyen, *Sci. Eng*. C, 2013, **4**, 2229.

24 H. Niu, Q. Chen, H. Zhu, Y. Lin and X. Zhang, *J. Mater. Chem*, 2003, **13**, 1803.

25 A.Y. Yermakov, T.A. Feduschak, V.S. Sedoi, M.A. Uimin and A.A. Mysik, *J. Magn. Magn. Mater*, 2004, **272**, 2445.

26 V.O. Saik and S. Lipsky, *Chem. Phys. Lett*, 1997, **264**, 649.

27 V.B. Ukraintsev, V.A. Matsura, V.V. Potekhin, V.V. Platonov, O.M. Tatsenko and K.A. Khokhryakov, *Russ. J. Gen. Chem*, 2005, **75**, 1260.

28 H. Niu, Q. Chen, M. Ning, Y.S. Jia and X.J. Wang*, J. Phys. Chem. B*, 2004, **108**, 3996.

29 J. Wang, Q. Chen, C. Zeng and B. Hou, *Adv. Mater*, 2004, **16**, 137.

30 L. Zhang, J. Luo and Q. Chen, *J. Phys.: Condens. Matter*, 2005, **17**, 5095.

View Article Online
DOI: 10.1039/C5RA14467A

31 G. Cheng, D. Romero, G.T. Fraser and A.R. Hight Walker, *Langmuir*, 2005, **21**, 12055.

32 J. Wang, Q. Chen and S. Che, *J. Magn. Magn. Mater*, 2004, **280**, 281.

33 A.Y. Yermakov, T.A. Feduschak, M.A. Uimin, A.A.; Mysik, V.S. Gaviko, O.N. Chupakhin, A.B. Shishmakov, V.G.; Kharchuk, L. A. Petrov, L.A. Kotov, A.V. Vosmerikov and A.V. Korolyov, *Solid State Ionics*, 2004, **172**, 317.

34 S. Kitashima, A. Kuroda, K. Hirose, M. Senna, A. Y. Yermakov and M.A. Uimin, *J. Alloys Compd*, 2007, **434**, 646.

35 J. Sá, J. Szlachetko, M. Sikora, M. Kavcic, O.V. Safonova and M. Nachtegaal, *Nanoscale*, 2013, **5**, 8462.

36 P. Lin, J. Peng, B. Hou and Y. Fu, *J. Phys. Chem*, 1993, **97**, 1471.

37 G.H. Yao, F. Wang, X.B. Wang and K.T. Gui, *Energ*, 2010, **35**, 2295.

38 E. Rafiee, H. Mahdavi and M. Joshaghani, *Mol. Divers*, 2011, **15**, 125.

39 X.L. Tang, H.W. Zhang, H. Su, Z.Y. Zhong and Y.l. Jing, *J. Solid. State. Chem.*, 2006, **179**, 1618.

40 D. Hua, Y. Wang and Q. Song, *Particuology*, 2009, **7**, 363.

41 S. Xuan, Y.X.J. Wang, K.C.F. Leung and K. Shu, *J. Phys. Chem. C*, 2008, **112**, 18804.

42 M. Ishii, M. Nakahira and T. Yamanaka. *Solid State Commn*, 1972, **11**, 209.

43 J. Wang, Q. Chen, C. Zeng and B. Hou, Adv. Mater, 2004, **16**, 137.

44 K. Sivakumar, A. Kathirvel and A. Lalitha, *Tetrahedron. Lett*, 2010, **51**, 3018.

45 M.A. Pasha and A. Nizam, *J. Saudi Chem. Soc*, 2011, **15**, 55.

46 J. Kienberger, N. Noormofidi, I. Mühlbacher, I. Klarholz, C. Harms and Ch. Slugovc, *Polym. Chem*, 2012, **50**, 2236.

47 S. Rostamnia and A. Zabardasti, *J. Fluorine. Chem*, 2012, **144**, 69.

48 S. Samai, G.C. Nandi, P. Singh and M.S. Singh, *Tetrahedron*, 2009, **65,** 10155.

49 S.D. Sharma, P. Hazarika and D. Konwar, *Tetrahedron. Lett*, 2008, **49**, 2216.

50 A.R. Khosropour, *Ultrason. Sonochem*, 2008, **15**, 659.

51 A.A. Marzouk, V.M. Abbasov, A.H. Talybov and S.K. Mohamed, *World Res J Org Chem*, 2013, **1**, 6.

52 K. Ramesh, S. Narayana Murthy, K. Karnakar, Y.V.D. Nageswar, K. Vijayalakhshmi, B.L.A.P. Devi, and R.B.N. Prasad, *Tetrahedron. Lett*, 2012, **53**, 1126.

53 M.V. Chary, N.C. Keerthysri, S.V.N. Vupallapati, N. Lingaiah and S. Kantevari, *Catal. Comm*, 2008, **9**, 2013.

54 B.P. Bandgar, B.S. Hote, B.L. Korbad and S.A. Patil, *E-J. Chem*, 2011, **8**, 1339.

55 M.G. Shen, C. Cai and W.B. Yi, *J. Fluorine. Chem*, 2008, **129**, 541.

56 A.R. Khosropour, *J. Chem*, 2008, **86**, 264.

57 L. Kong, X. Lv, Q. Lin, X. Liu, Y. Zhou and Y. Jia, *Org. Process. Res, Dev*. 2010, **14**, 902.

58 N. Khodabakhsh, M.M.R. Mirzaee, S. Dariush and D. Saberi, *Chin. J. Chem*, 2010, **28**, 663.

59 C. Zhang, E.J. Moran, T.F. Woiwode, K.M. Short and A.M.M. Mjalli, *Tetrahedron. Lett*, 1996, **37**, 751.

60 S.E. Wolkenberg, D.D. Wisnoski, W.H. Leister, Y. Wang, Z. Zhao and C.W. Lindsley, *Org. Lett*, 2004, **6**, 1453.

61 J. Safari and Z. Zarnegar, *Ultrason. Sonochem*, 2013, **20**, 740.

62 M.V. Reddy and Y.T. Jeong, *J. Fluorine. Chem*, 2012, **142**, 45.

63 D. Kumar, D.N. Kommi, N. Bollineni, A.R. Patel and A.K. Chakraborti, *Green Chem*, 2012, **14**, 2038.

64 R.K. Sharma and C. Sharma, *Catal. Commun*, 2011, **12**, 327.

65 A. Shaabani, A. Rahmati, E. Farhangi and Z. Badri, *Catal. Commun*, 2007, **8**, 1149.

66 Z.H. Zhang, H.Y. Lu, S.H. Yang and J.W. Gao, *J. Comb. Chem*, 2010, **12**, 643.

67 A. Teimouri and A. Najafi Chermahini, *J. Mol. Catal. A: Chem*, 2011, **346**, 39.

68 S.V. Bhosale, M.B. Kalyankar, S.V. Nalage, D.S. Bhosale, S.L. Pandhare, T.V. Kotbagi, Sh.B. Umbarkar and M.K. Dongare, *Synthetic. Commun*, 2011, **41**, 762.